nature COMMUNICATIONS

ARTICLE

Received 10 Mar 2013 | Accepted 11 Sep 2013 | Published 8 Nov 2013

DOI: 10.1038/ncomms3596

Enhanced spin-triplet superconductivity near dislocations in Sr_2RuO_4

Y.A. Ying[1], N.E. Staley[1], Y. Xin[2], K. Sun[3,4], X. Cai[1], D. Fobes[5], T.J. Liu[5], Z.Q. Mao[5] & Y. Liu[1,6]

Superconductors with a chiral *p*-wave pairing are of great interest because they could support Majorana modes that could enable the development of topological quantum computing technologies that are robust against decoherence. Sr_2RuO_4 is widely believed to be a chiral *p*-wave superconductor. Yet, the mechanism by which superconductivity emerges in this, and indeed most other unconventional superconductors, remains unclear. Here we show that the local superconducting transition temperature in the vicinity of lattice dislocations in Sr_2RuO_4 can be up to twice that of its bulk. This is all the more surprising for the fact that disorder is known to easily quench superconductivity in this material. With the help of a phenomenological theory that takes into account the crystalline symmetry near a dislocation and the pairing symmetry of Sr_2RuO_4, we predict that a similar enhancement should emerge as a consequence of symmetry reduction in any superconductor with a two-component order parameter.

[1] Department of Physics and Materials Research Institute, The Pennsylvania State University, University Park, Pennsylvania 16802, USA. [2] National High Magnetic Field Laboratory, Florida State University, Tallahassee, Florida 32310, USA. [3] Department of Physics, University of Maryland, Condensed Matter Theory Center and Joint Quantum Institute, College Park, Maryland 20742, USA. [4] Department of Physics, University of Michigan, Ann Arbor, Michigan 48109, USA. [5] Department of Physics, Tulane University, New Orleans, Louisiana 70118, USA. [6] Department of Physics and Astronomy and Key Laboratory of Artificial Structures and Quantum Control (Ministry of Education), Shanghai Jiao Tong University, Shanghai 200240, China. Correspondence and requests for materials should be addressed to Y.L. (email: liu@phys.psu.edu).

Sr_2RuO_4 has attracted much attention recently because it may feature a pairing state hosting Majorana bound states useful for topological quantum computing[1–3]. A large body of experimental data, including that obtained in phase-sensitive measurements[4], has shown that the layered perovskite Sr_2RuO_4 is a spin-triplet, odd-parity superconductor[5,6]. Assuming that superconductivity in this material is two-dimensional in nature, the fourfold tetragonal crystalline symmetry dictates that the pairing symmetry must be one of the five representations[7]. Among those, only the two-component, $p_x \pm ip_y$ state is consistent with the muon spin rotation[8] and Kerr rotation[9] measurements that suggest the presence of a spontaneous magnetic field in the superconducting state of Sr_2RuO_4, making it an electronic analogue[7] of the superfluid ^{3}He A-phase, and a chiral p-wave superconductor for which a Majorana zero-energy mode bound to the normal core of a half-flux quantum vortex has been predicted[1,2]. An important question of interest is what is the microscopic mechanism responsible for such a highly exotic superconducting state. In this regard, models based on ferromagnetic[10] or antiferromagnetic fluctuations[11], spin-orbit coupling[12], interaction theory[13,14], Hund's rule coupling[15] and interplay of charge and spin fluctuations in the one-dimensional bands[16] have been proposed. The debate on these mechanisms is currently ongoing[6].

The eutectic phase of Sr_2RuO_4-Ru featuring crystalline islands of Ru embedded in the bulk crystalline Sr_2RuO_4, found previously to feature a superconducting transition temperature (T_c) nearly double than that of the bulk Sr_2RuO_4 (ref. 17), may provide insight into the mechanism issue. The T_c enhancement was attributed to the capillary effect at the Ru/Sr_2RuO_4 interface[18]. It was more recently suggested that the enhanced superconductivity occurs on the Sr_2RuO_4 side away from[19] rather than at the Ru/Sr_2RuO_4 interface as assumed previously[18]. Meanwhile, dislocations were found to be abundant, which led to the intriguing question as to whether these dislocations are the origin of the enhancement of T_c[19]. The bulk eutectic phase of Sr_2RuO_4-Ru possesses both Ru/Sr_2RuO_4 interfaces and dislocations (Fig. 1a), making it difficult to separate the effect of dislocations from that of the interfaces. Single-crystal flakes of Sr_2RuO_4 prepared by mechanical exfoliation, in which islands of Ru and dislocations can be identified by scanning electron microscopy (SEM) and/or transmission electron microscopy (TEM; Fig. 1b), provide an opportunity to study separately the respective effect of the Sr_2RuO_4/Ru interface and dislocations (see below). Interestingly, an edge dislocation in a Sr_2RuO_4 lattice (Fig. 1c) is expected to possess complicated modifications to the local crystalline structure and electronic states, which may lead to a new way of hosting a Majorana zero mode[20]. Nevertheless, it has a dominating overall feature that the fourfold rotational symmetry is lowered to one that is basically twofold.

Here we report our observation of the enhancement in local T_c near lattice dislocations in Sr_2RuO_4 up to about twice of the bulk. We develop a phenomenological theory to describe the observation and predict that the enhanced T_c is ubiquitous for symmetry reduction in superconductors with a two-component order parameter.

Results

Phenomenology. A phenomenological theory can be formulated to capture the effect of the symmetry reduction. The general free-energy density of the bulk Sr_2RuO_4 with a fourfold tetragonal symmetry in zero magnetic field can be written as[18],

$$\begin{aligned} f =& a\left(|\eta_x|^2+|\eta_y|^2\right)+b_1\left(|\eta_x|^2+|\eta_y|^2\right)^2+\frac{b_2}{2}\left(\eta_x^{*2}\eta_y^2+c.c.\right)\\ &+b_3\,|\eta_x|^2|\eta_y|^2+K_1\left(|\partial_x\eta_x|^2+|\partial_y\eta_y|^2\right)+K_2\left(|\partial_y\eta_x|^2+|\partial_x\eta_y|^2\right)\\ &+\left[K_3(\partial_x\eta_x)^*\left(\partial_y\eta_y\right)+K_4(\partial_y\eta_x)^*\left(\partial_x\eta_y\right)+c.c.\right]+K_5\left(|\partial_z\eta_x|^2+|\partial_z\eta_y|^2\right) \end{aligned} \quad (1)$$

where η_x and η_y denote the two-component order parameter, $a(T)=\alpha(T-T_{c0})$, with α a constant and $T_{c0}=1.5$ K the bulk T_c of Sr_2RuO_4, b_i ($i=1$–3) and K_j ($j=1$–5) parameters characterizing the bulk superconductor. The effect of the symmetry lowering near a dislocation can be illustrated by first considering a bulk Sr_2RuO_4 crystal. When an in-plane uniaxial strain is applied to the crystal, the lattice distortion leads naturally to a structural distortion and change in the electronic band structure, which may in turn cause the T_c to change. Without getting into the analysis of the complicated microscopic effect, we will write down a phenomenological theory featuring a set of phenomenological parameters, m_1 and m_2 used to quantify the effect of structural distortions and μ to measure the hybridization of the two-order parameter components, describing the symmetry-breaking strength.

To obtain only the highest superconducting transition temperature (T_{ch}), it is sufficient to consider the free-energy density up to the quadratic terms. We assume a spatially uniform-order parameter, for which the gradient terms vanish. Therefore, following the idea of degenerate perturbation theory, the free-energy density describing the reduced symmetry (f_{RS}) can be written as[21,22]

$$\begin{aligned} f_{RS} =& (a+m_1)|\eta_x|^2+(a+m_2)\,|\eta_y|^2\\ &+\mu\eta_x^*\eta_y+\mu^*\eta_x\eta_y^*+\sum_{ijkl}\Gamma_{ijkl}\eta_i^*\eta_j^*\eta_k\eta_l \end{aligned} \quad (2)$$

The modified transition temperature T_{ch}, determined by the eigenvalues of the quadratic terms, is given by

$$T_{ch}=T_{c0}+\frac{1}{\alpha}\left(\sqrt{m_-^2+|\mu|^2}-m_+\right) \quad (3)$$

where $m_\pm=(m_1\pm m_2)/2$. Equation (3) indicates that the asymmetry-related terms m_- and μ always enhance T_{ch} in one superconducting channel, whereas reduce it in the other. In general, the level of crystalline distortion m_+ may either enhance or suppress the transition temperature. For certain parameters, the symmetry-lowering effect dominates and $T_{ch}>T_{c0}$ can be obtained (Fig. 1d).

The above consideration may be extended to the analysis of a bulk crystal of Sr_2RuO_4 possessing a single dislocation (Fig. 1c). If the dislocation line features a width d in the x direction, we may obtain the local T_c from T_{ch} (m_1, m_2 and μ) in the above treatment of a bulk crystal subjecting to a uniaxial stress. The effect of the bulk on the embedded dislocation region in this approach is described by a δ-function in the free-energy density

$$f_I=\delta(x)d\alpha(T-T_{ch})\left(|\eta_x|^2+|\eta_y|^2\right) \quad (4)$$

as done previously to account for the capillary effect at the interface between Ru and Sr_2RuO_4 (ref. 18). Solving the linearized Ginzburg–Landau equations derived from equation (1) and matching the boundary conditions at $x=0$ (see Methods), we found that T_c is given by the solution of

$$2\sqrt{\frac{K_2}{\alpha}(T_c-T_{c0})}=d(T_{ch}-T_c) \quad (5)$$

which requires that $T_{ch}>T_c>T_{c0}$ for self consistency. The spatial dependence of the order parameter was found to be symmetric with respect to the dislocation line at $x=0$, with the order parameter reaching a maximum value at the dislocation below T_c. As the highest transition temperature found in any Sr_2RuO_4 including eutectic systems is 3.2 K (ref. 6), we assume that $T_{ch}=3.2$ K. As a result, the experimentally observed typical onset T_c of 2.5 K corresponds to $d=3.5(K_2/\alpha T_{c0})^{1/2}$. This d-value is comparable to the superconducting coherence length given by

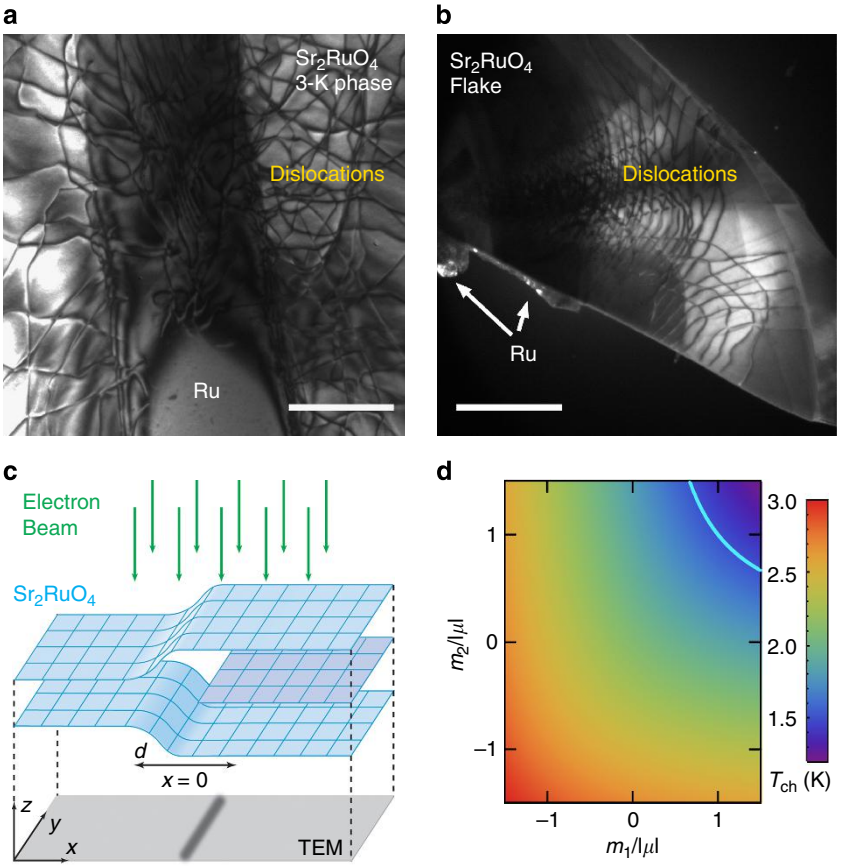

Figure 1 | Dislocations and prediction of an enhanced T_c. (**a**) Transmission electron microscopy (TEM) image of a Sr_2RuO_4-Ru eutectic crystal showing a Ru island in the middle and large numbers of dislocations. (**b**) TEM image of a Sr_2RuO_4 single-crystal flake, showing dislocations and nanodomains of Ru on the edge. The dislocation lines are the superposition of many layers. Scale bars, 500 nm. (**c**) Schematic of an edge dislocation caused by an extra layer (purple) in a Sr_2RuO_4 lattice, indicating that the local fourfold rotational symmetry is broken. The edge dislocation scatters the electron beam in a TEM study, manifesting itself as a dark line in the TEM image. (**d**) T_{ch} plotted as a function of $m_1/|\mu|$ and $m_2/|\mu|$ for $|\mu|/\alpha T_{c0} = 0.4$. The value of T_{ch} is represented by a colour scale. The highlighted curve represents the contour of $T_{ch} = 1.5$ K.

$\xi_{1,2}(0) = (K_{1,2}/\alpha T_{c0})^{1/2}$ for the anisotropic stripe, suggesting that the use of a δ-function is self-consistent, given that the basic length for order parameter variation in the Ginzburg–Landau theory is $\xi_{1,2}(0)$. It is interesting to note that similar phenomenology can be obtained if two pairing states represented by a single-component order parameter have identical or very close intrinsic T_c. We note that the above theory is not applicable for a point defect for which the perturbation to local crystalline structure is essentially isotropic (rotationally invariant).

The main predictions of our phenomenological theory are threefold. First, an enhanced T_c can be obtained if the symmetry reduction effect dominates over other effects from the presence of a dislocation; second, the resulting local T_c depends strongly on the parameters characterizing the symmetry reduction, suggesting that the local T_c may vary from dislocation to dislocation; third, the magnitudes of the two components of the superconducting order parameter near a dislocation may depend on the temperature differently, leading to a change in the pairing symmetry as the temperature is lowered (see below).

Electrical transport. Single-crystal flakes of Sr_2RuO_4 were selected under optical microscope and examined by SEM before device fabrication. Some flakes were also examined by TEM. Dislocations and Ru nanodomains can be identified. Ru nanodomains (if observed) appear to always locate at the edge of the crystal (Fig. 1b), perhaps because cleaving tends to occur at the Ru/Sr_2RuO_4 boundary because of a reduced mechanical strength. For most flakes, however, SEM imaging did not show any Ru nanodomains. These Ru-free flakes of Sr_2RuO_4 were used to prepare four-point devices for electrical transport measurements. In particular, the temperature dependence of the resistivity for sample A (Fig. 2a) shows an onset T_c of 1.45 K (Fig. 2b), very close to the optimal T_c of Sr_2RuO_4. For sample B, SEM imaging revealed no Ru nanodomains (Fig. 2d) before the low-temperature transport measurement. However, transport measurements showed an onset T_c of 2.8 K (Fig. 2f). TEM studies of the same device after the transport measurements confirmed the absence of Ru nanodomains and further revealed the presence of dislocations between the two voltage leads (Fig. 2e). Similar results were obtained in sample C (Fig. 2g,h) with onset $T_c = 1.9$ K (Fig. 2i). The magnetic field dependence of the resistivity for field applied along the c axis was also measured. It was found that the upper critical field (H_{c2}) is 50 mT for sample A (Fig. 2c), comparable to that of the pure phase (75 mT), whereas sample C showed an H_{c2} of 0.3T (inset of Fig. 2i), closer to that of the eutectic phase[5,6]. Therefore, our experimental observations provide a direct confirmation that the presence of dislocations leads to the enhancement of T_c in Sr_2RuO_4 as predicted by the theory.

The presence of multiple dislocations in our sample, which should be described by different sets of symmetry reduction parameters, should result in multiple phases in the samples with

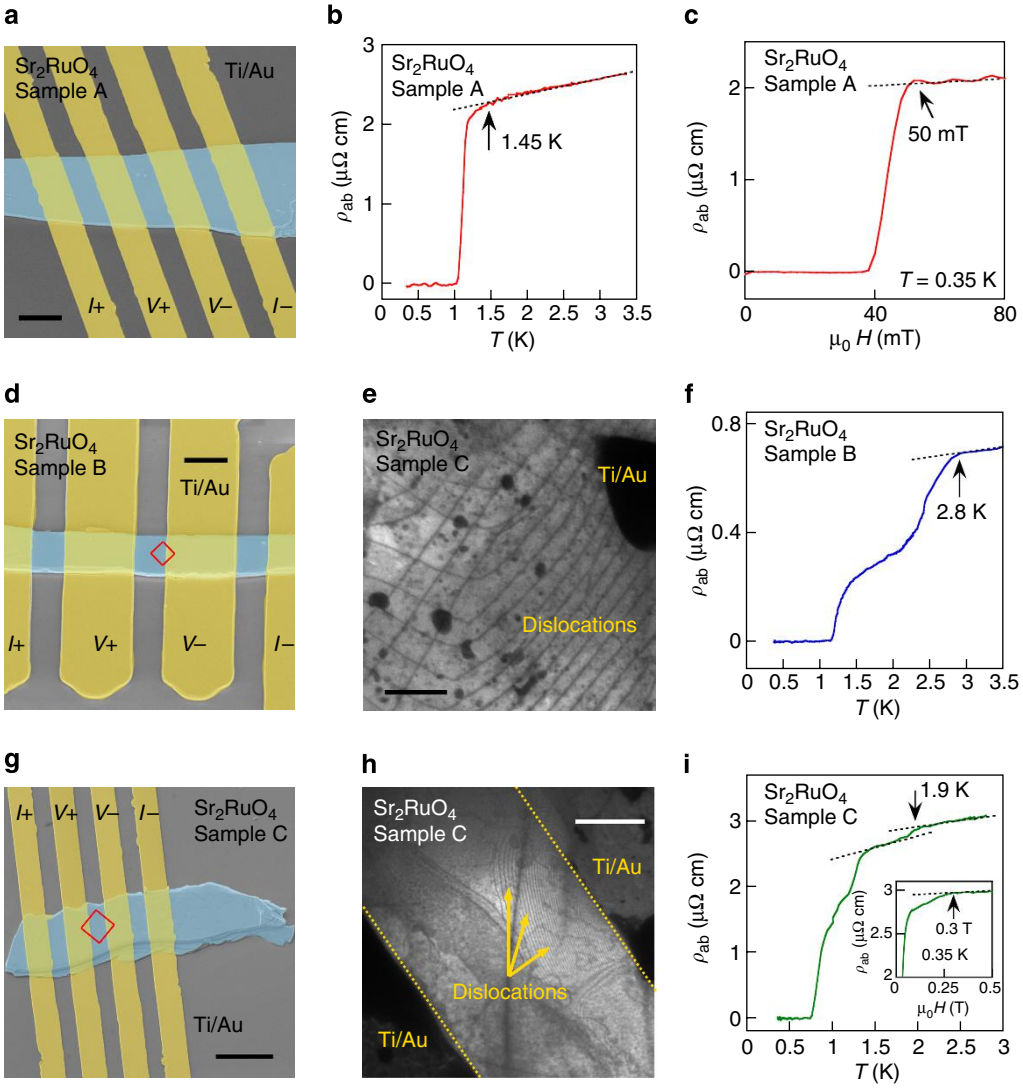

Figure 2 | Observation of an enhanced T_c with dislocations. (**a**) False-colour SEM image of sample A. Scale bar, 5 μm. (**b**) Temperature dependence of the in-plane resistivity ρ_{ab} for sample A, taken at zero applied magnetic field. (**c**) Magnetic field dependence of ρ_{ab} for sample A. (**d**) False-colour SEM image of sample B. The red square indicates the area examined by TEM. Scale bar, 5 μm. (**e**) TEM image of the boxed area in **d** for sample B, showing dislocation lines but no Ru nanodomains. Scale bar, 200 nm. The regions not shown in this image were also checked by TEM and found to possess no Ru nanodomains. (**f**) Zero-field $\rho_{ab}(T)$ for sample B. (**g**) False-colour SEM image of sample C. The red square indicates the area examined by TEM. Scale bar, 10 μm. (**h**) TEM image of the boxed area in **g** for sample C. Scale bar, 1 μm. (**i**) Zero-field $\rho_{ab}(T)$ for sample C. Inset: $\rho_{ab}(H)$ for sample C. In the above line plots, the dashed lines indicate a linear fit of the normal-state resistivity. The deviation from such a fit defines the onset T_c and upper critical field.

enhanced T_c. This is indeed consistent with the multiple features observed in the $\rho_{ab}(T)$ curves (Fig. 2f,i). Further, the voltage–current (V–I) characteristics and the dV/dI–I curves were found to show double features suggesting the existence of two different phases at low temperatures in sample C (Fig. 3a), one corresponding to the dislocations and the other the bulk phase. In contrast, in sample A, a single onset T_c (Fig. 2b) and a single feature (Fig. 3b) were found in the $\rho_{ab}(T)$, and V–I and dV/dI–I curves, respectively.

Tunnelling. In addition to an enhanced T_c and inhomogeneous superconducting phase, the phenomenological theory presented above also predicts that the relative magnitude of the two components of the superconducting order parameter varies strongly as the temperature is lowered. In particular, for a system with an onset T_c of 2.5 K, the y component of the order parameter η_y was calculated (see Methods) and found to be much larger than the x component η_x above T_{c0} (Fig. 4a, upper panels) at 1.9 K (below T_c). On the other hand, the two components become comparable below T_{c0} (Fig. 4a, lower panels). Therefore, the local density of states (DOSs) near a dislocation should vary accordingly as the temperature is lowered.

The experimental detection of the temperature dependence of the order parameter near a dislocation is a significant challenge. Ideally, a local probe such as a scanning tunneling microscope with tunneling spectroscopy capability can be used to probe the local superconducting order parameter. However, as a surface probe, a scanning tunneling microscope cannot locate a dislocation embedded inside the crystal. We performed quasi-particle tunneling measurements on a tunnel junction of Sr_2RuO_4-TiAl fabricated on a Ru-free flake. Tunneling spectra obtained at an in-plane magnetic field of 40 mT, at which the superconductivity in Al counter electrodes is suppressed, feature zero-bias conductance peaks (ZBCPs). Such ZBCPs were observed in Sr_2RuO_4 previously[23,24], and linked to the p-wave

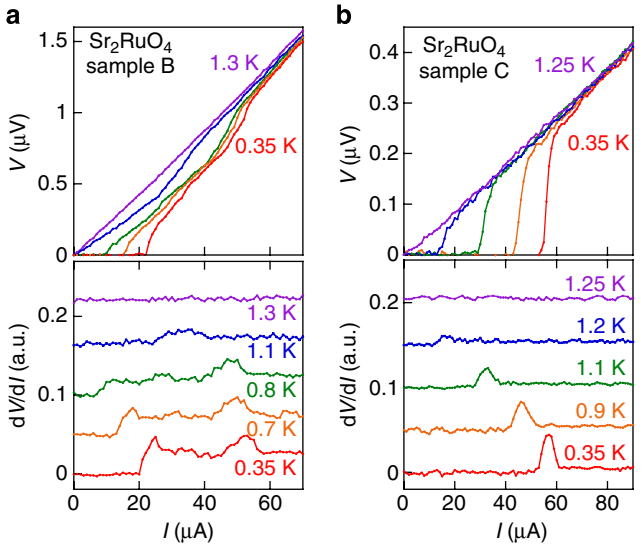

Figure 3 | Observation of multiple superconducting phases. Zero-field *V*–*I* curves and corresponding d*V*/d*I*–*I* curves at various temperatures for (**a**) sample C showing multiple transitions and (**b**) sample A showing a single transition. The d*V*/d*I*–*I* curves except for those at 0.35 K were shifted for clarity.

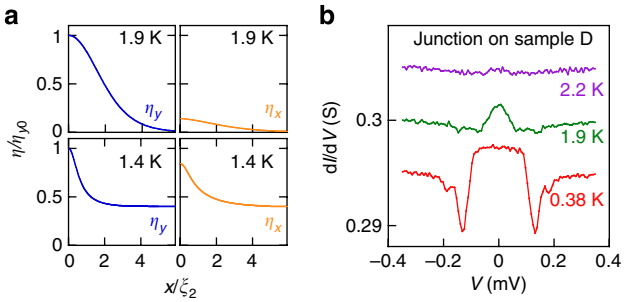

Figure 4 | Variations of the superconducting order parameter as a function of temperature. (**a**) Spatial dependence of η_x and η_y normalized to the value of η_y at $x=0$ for $T_1=1.9$ K and $T_2=1.4$ K. Other parameters are $T_{c0}=1.5$ K, $T_{ch}=3.2$ K, $T_c=2.5$ K and $\xi_2(T_{1,2})=[K_2/|\alpha(T_{1,2}-T_{c0})|]^{1/2}$, superconducting coherence lengths at finite temperatures. (**b**) Quasiparticle tunneling spectra obtained from the junction on sample D, showing a ZBCP below 2.2 K. The ZBCP at 1.9 K shows a triangular shape, whereas that at 0.38 K shows a rectangular shape.

pairing symmetry. For sample D (onset $T_c=2.5$ K), the ZBCP was visible at 2.2 K, with its shape varying as the temperature is lowered (Fig. 4b). The triangularly shaped ZBCP seen at 1.9 K is particularly akin to those found previously in the break junctions of Sr_2RuO_4-Ru eutectic crystals above 1.5 K (ref. 23) and is consistent with the expectations of our phenomenological theory that predicts that the η_y component dominates at 1.9 K with a nearly zero η_x component. On the other hand, the ZBCP found at 0.38 K has a rectangular shape, with an onset of superconducting energy gap feature around 0.2 meV, consistent with the weak-coupling value for a T_c of 1.5 K and an order parameter with two equal-magnitude components.

Discussion

The crystalline symmetry lowering characterized by the phenomenological parameters manifests itself microscopically as lattice distortions. An edge dislocation demands the existence of both a compressed region and a stretched region extending along the dislocation line (Fig. 1c), allowing extended regions of distortions to occur. It is relevant to note a recent uniaxial pressure study on pure Sr_2RuO_4 that revealed an enhancement of T_c up to 3.2 K (onset) and emergence of a continuous distribution of local T_c[25]. The enhancement of T_c observed in that experiment can be interpreted as a consequence of enhanced interlayer coupling. Indeed, the quantum oscillation measurements carried out under a hydrostatic pressure[26] suggest that the pressure, which lowers T_c of Sr_2RuO_4, makes the Fermi surface more two-dimensional like, implying that weakening the interlayer coupling reduces T_c, consistent with the uniaxial strain result. Meanwhile, the compressed region near a dislocation favours an increased interlayer coupling, suggesting that the observed enhanced T_c in Sr_2RuO_4 near a dislocation may have its origin also in the strengthening of interlayer coupling.

Electronically, the symmetry lowering could also lead to changes in the DOSs near the Fermi level as well as the average pairing interaction evaluated over the perturbed Fermi surface, both of which may cause the T_c to vary. The change in the DOSs may favour pairing in a specific channel that will result enhancement of T_c for that channel, although the pairing interaction that depends on the exact mechanism is yet to be fully understood. The perturbation on the electronic states by a dislocation should be band dependent, which suggests that our result may have implications on the multiple-band superconductivity picture of Sr_2RuO_4 (refs 16,27). The implications of our results on other proposed mechanisms for superconductivity in Sr_2RuO_4, such as incommensurate fluctuations[11] or Coulomb interactions[13,14], need to be further clarified.

Our experimental results on Ru-free flakes of Sr_2RuO_4 are in agreement with the phenomenological theory, providing the first demonstration of symmetry reduction-induced T_c enhancement near a dislocation in a spin-triplet superconductor featuring a two-component order parameter. Our findings have raised an intriguing question on whether it is possible to use symmetry reduction to raise T_c in other exotic superconductors described by a two-component superconducting order parameter. This may also be relevant to multiband superconductors for which the magnitudes of the order parameter on different bands are comparable. More experiments are needed to establish this possibility.

Methods

Phenomenological theory. To solve the linearized Ginzburg–Landau equations on the stripe, we adopt constrains for K_j used in ref. 18, $K_1/3=K_2=K_3=K_4\gg K_5$. In the geometry we consider, the problem can be simplified into a one-dimensional problem by ignoring the variations along the *y* and *z* axis. To examine the onset T_c, we consider the linearized Ginzburg–Landau equations derived from equation (1)

$$K_1\partial_x^2\eta_x - a\eta_x = 0 \quad (6)$$

$$K_2\partial_x^2\eta_y - a\eta_y = 0 \quad (7)$$

for $x\neq 0$. For $x=0$, we assume a fully transparent boundary at which the solutions have to be continuous. Meanwhile, the solutions satisfy the boundary conditions derived from equation (4)

$$K_1\partial_x\eta_x|_{x=0+} - K_1\partial_x\eta_x|_{x=0-} - \alpha d(T-T_{ch})\eta_x = 0 \quad (8)$$

$$K_2\partial_x\eta_y|_{x=0+} - K_2\partial_x\eta_y|_{x=0-} - \alpha d(T-T_{ch})\eta_y = 0 \quad (9)$$

The solutions for temperatures above T_{c0} have the following forms

$$\eta_x = \eta_{x0}\exp(-x/\xi_1) \quad \text{for } x>0 \quad (10)$$

$$\eta_x = \eta_{x0}\exp(x/\xi_1) \quad \text{for } x<0 \quad (11)$$

where $\xi_1(T)=(K_1/|a|)^{1/2}$.

$$\eta_y=\eta_{y0}\exp(-x/\xi_2) \quad \text{for } x>0 \tag{12}$$

$$\eta_y=\eta_{y0}\exp(x/\xi_2) \quad \text{for } x<0 \tag{13}$$

where $\xi_2(T)=(K_2/|a|)^{1/2}$. Matching the boundary conditions equations (8) and (9), we obtain the following equations

$$2\sqrt{K_1\alpha(T-T_{c0})}+\alpha d(T-T_{ch})=0 \tag{14}$$

$$2\sqrt{K_2\alpha(T-T_{c0})}+\alpha d(T-T_{ch})=0 \tag{15}$$

Note that if $T_{ch}>T_{c0}$, we always have a solution T_c such that $T_{ch}>T_c>T_{c0}$. Meanwhile, because $K_1/3=K_2$, equation (15) gives a higher instability temperature, indicating that the y component becomes non-zero first.

To obtain the spatial dependence of the order parameters, we numerically solve the Ginzburg–Landau equations by taking the phenomenological parameters $2b_1=3b_2=-3b_3=0.4\alpha$, $T_{ch}=3.2$ K, $K_1/\alpha T_{c0}=3K_2/\alpha T_{c0}=1$, the same as those used in ref. 18. We expand the δ-function in equation (4) into a Gaussian function. The Ginzburg–Landau equations then read

$$K_1\partial_x^2\eta_x-\alpha(T-T_{c0})\eta_x-\frac{\alpha(T-T_{ch})}{\sqrt{2\pi}}e^{-\frac{x^2}{2d^2}}\eta_x-2b_1(\eta_x^2+\eta_y^2)\eta_x=0 \tag{16}$$

$$K_2\partial_x^2\eta_y-\alpha(T-T_{c0})\eta_y-\frac{\alpha(T-T_{ch})}{\sqrt{2\pi}}e^{-\frac{x^2}{2d^2}}\eta_y-2b_1(\eta_x^2+\eta_y^2)\eta_y=0 \tag{17}$$

where $d=3.5(K_2/\alpha T_{c0})^{1/2}=2$, giving rise to $T_c=2.5$ K. When x goes to infinite, the solutions decay to zero for $T>1.5$ K and approach a constant of $\eta_x=\eta_y=(-a/4b_1)^{1/2}$ for $T<1.5$ K. The results are plotted in Fig. 4a.

Material. Easily cleavable single crystals of Sr_2RuO_4 were synthesized by the floating-zone method. Because of the high vapour pressure of RuO_2, excess Ru needs to be added to form a crystal with the correct atomic ratio. In the crystal we used, 10% excess Ru (a reduced amount of Ru overcompensation) was added in the starting rod to suppress the formation of Sr_2RuO_4-Ru and Sr_2RuO_4-$Sr_3Ru_2O_7$ eutectic phases, both of which were found previously to possess an enhanced T_c[17,28]. A bulk crystal from this batch was measured and showed a broad transition with a bulk T_c around 1.35 K, slightly lower than the optimal T_c for Sr_2RuO_4. Given that the same starting material with proper Ru overcompensation does yield crystals of Sr_2RuO_4 with optimal T_c, the slightly suppressed bulk T_c value is due to structural imperfection rather than an elevated impurity levels in the crystals. Indeed, devices made on flakes of Sr_2RuO_4 can show an onset T_c very close to the optimal. The use of easily cleavable Sr_2RuO_4 crystals is necessary for this study as superconducting films of Sr_2RuO_4 are not available, despite an early report of initial synthesis success[29].

To make a TEM sample of Sr_2RuO_4 flakes, a bulk Sr_2RuO_4 crystal was sonicated in methanol. Droplets containing tiny flakes of Sr_2RuO_4 were dripped onto a TEM grid with carbon membrane. After the methanol dried, Sr_2RuO_4 flakes remained on the carbon membrane. Thin flakes that are electron-transparent were searched and studied by TEM. Flakes with Ru nanodomains on the edge and a large amount of dislocation lines were observed (Fig. 1b).

Device fabrications. We prepared single-crystal flakes with a lateral dimension of roughly 10–50 μm and a thickness of 300–800 nm by mechanical exfoliation. The flakes were transferred onto a Si/SiO_2 substrate with the c axis of the crystal perpendicular to the substrate. A standard four-point probe was prepared by contact photolithography. Electrical leads of 50 nm Ti and 200 nm Au were deposited. After carrying out electric transport measurements at low temperatures, the flakes of sample B and C were further transferred onto a TEM grid using the standard tool of a tungsten tip. TEM study was then carried out on these two samples, revealing dislocations but no Ru nanodomains (Fig. 2e,h).

To fabricate quasiparticle tunneling devices on flakes, a few more steps than those for four-point transport devices were taken. In particular, 200-nm-thick SiO_2 was first deposited on top of the flakes as a protection layer. Focused ion beam of 30 kV Ga ions was used to carve ramps on the edge of the flakes. Twenty-minute ion mill of 300 V Ar ions was then used to take off the surface layer damaged by high-energy focused ion beam. After photolithography patterning, 5 nm Ti and 200 nm Al were deposited as a counter electrode. The thin Ti layer was used here to improve the adhesion of Al to Sr_2RuO_4.

Transport measurements. Low-temperature direct current measurements were performed in a ^{3}He refrigerator with a base temperature of 0.35 K. All leads entering the cryostat are shielded and filtered by low-pass resister-capacitor (RC) filters with a 3-dB cutoff frequency of 600 kHz.

References

1. Ivanov, D. A. Non-Abelian statistics of half-quantum vortices in p-wave superconductors. *Phys. Rev. Lett.* **86,** 268–271 (2001).
2. Das Sarma, S., Nayak, C. & Tewari, S. Proposal to stabilize and detect half-quantum vortices in strontium ruthenate thin films: non-Abelian braiding statistics of vortices in p_x+ip_y superconductor. *Phys. Rev. B* **73,** 220502(R) (2006).
3. Nayak, C., Simon, S. H., Stern, A., Freedman, M. & Das Sarma, S. Non-Abelian anyons and topological quantum computation. *Rev. Mod. Phys.* **80,** 1083–1159 (2008).
4. Nelson, K. D., Mao, Z. Q., Maeno, Y. & Liu, Y. Odd-parity superconductivity in Sr_2RuO_4. *Science* **306,** 1151–1154 (2004).
5. Mackenzie, A. P. & Maeno, Y. The superconductivity of Sr_2RuO_4 and the physics of spin-triplet pairing. *Rev. Mod. Phys.* **75,** 657–712 (2003).
6. Maeno, Y., Kittaka, S., Nomura, T., Yonezawa, S. & Ishida, K. Evaluation of spin-triplet superconductivity in Sr_2RuO_4. *J. Phys. Soc. Jpn* **81,** 011009 (2012).
7. Rice, T. M. & Sigrist, M. Sr_2RuO_4: an electronic analogue of ^{3}He? *J. Phys. Condens. Matter* **7,** L643–L648 (1995).
8. Luke, G. M. *et al.* Time-reversal symmetry breaking superconductivity in Sr_2RuO_4. *Nature* **394,** 558–561 (1998).
9. Xia, J., Maeno, Y., Beyersdorf, P. T., Fejer, M. M. & Kapitulnik, A. High resolution polar Kerr effect measurements of Sr_2RuO_4: evidence for broken time-reversal symmetry in the superconducting state. *Phys. Rev. Lett.* **97,** 167002 (2006).
10. Mazin, I. I. & Singh, D. J. Ferromagnetic spin fluctuation induced superconductivity in Sr_2RuO_4. *Phys. Rev. Lett.* **79,** 733–736 (1997).
11. Kuwabara, T. & Ogata, M. Spin-triplet superconductivity due to Antiferromagnetic spin-fluctuation in Sr_2RuO_4. *Phys. Rev. Lett.* **85,** 4586–4589 (2000).
12. Ng, K. K. & Sigrist, M. The role of spin-orbit coupling for the superconducting state in Sr_2RuO_4. *Europhys. Lett.* **49,** 473–479 (2000).
13. Nomura, T. & Yamada, K. Perturbation theory of spin-triplet superconductivity for Sr_2RuO_4. *J. Phys. Soc. Jpn* **69,** 3678–3688 (2001).
14. Koikegami, S., Yoshida, Y. & Yanagisawa, T. Superconductivity in Sr_2RuO_4 mediated by Coulomb scattering. *Phys. Rev. B* **67,** 134517 (2003).
15. Baskaran, G. Why is Sr_2RuO_4 not a high T_c superconductor? Electron correlation, Hund's coupling and p-wave instability. *Physica B* **223-224,** 490–495 (1996).
16. Raghu, S., Kapitulnik, A. & Kivelson, S. A. Hidden quasi-one-dimensional superconductivity in Sr_2RuO_4. *Phys. Rev. Lett.* **105,** 136401 (2010).
17. Maeno, Y. *et al.* Enhancement of superconductivity of Sr_2RuO_4 to 3K by embedded metallic microdomains. *Phys. Rev. Lett.* **81,** 3765–3768 (1998).
18. Sigrist, M. & Monien, H. Phenomenological thoery of the 3 Kelvin phase in Sr_2RuO_4. *J. Phys. Soc. Jpn* **70,** 2409–2418 (2001).
19. Ying, Y. A. *et al.* Suppression of proximity effect and the enhancement of p-wave superconductivity in the Sr_2RuO_4-Ru system. *Phys. Rev. Lett.* **103,** 247004 (2009).
20. Hughes, T. L., Yao, H. & Qi, X.-L. Majorana zero modes in dislocations of Sr_2RuO_4. Preprint at http://arXiv.org/abs/1303.1539 **1303,** 1539 (2013).
21. Sigrist, M., Joynt, R. & Rice, T. M. Behavior of anisotropic superconductors under uniaxial stress. *Phys. Rev. B* **36,** 5186 (1987).
22. Volovik, G. E. Splitting of the superconducting transition in high-temperature superconductors due to a slight orthorhombic nature. *JETP Lett.* **48,** 41–44 (1988).
23. Mao, Z. Q., Nelson, K. D., Jin, R., Liu, Y. & Maeno, Y. Observation of Andreev surface bound states in the 3-K phase region of Sr_2RuO_4. *Phys. Rev. Lett.* **87,** 037003 (2001).
24. Kashiwaya, S. *et al.* Edge states of Sr_2RuO_4 detected by in-plane tunneling spectroscopy. *Phys. Rev. Lett.* **107,** 077003 (2011).
25. Kittaka, S., Taniguchi, H., Yonezawa, S., Yaguchi, H. & Maeno, Y. Higher-T_c superconducting phase in Sr_2RuO_4 induced by uniaxial pressure. *Phys. Rev. B* **81,** 180510(R) (2010).
26. Forsythe, D. *et al.* Evolution of Fermi-liquid interactions in Sr_2RuO_4 under pressure. *Phys. Rev. Lett.* **89,** 166402 (2002).
27. Zhitomirsky, M. E. & Rice, T. M. Interband proximity effect and nodes of superconducting gap in Sr_2RuO_4. *Phys. Rev. Lett.* **87,** 057001 (2001).
28. Shiroka, T. *et al.* μSR studies of superconductivity in eutectically grown mixed ruthenates. *Phys. Rev. B* **85,** 134527 (2012).
29. Krockenberger, Y. *et al.* Growth of superconducting Sr_2RuO_4 thin films. *Appl. Phys. Lett.* **97,** 082502 (2010).

Acknowledgements

We acknowledge the useful discussions with S.B. Chung, Y. Maeno, C.C. Tsuei and V. Varkaruk. The work at Penn State is supported by DOE under Grant number DE-FG02-04ER46159. The nanofabrication part of the work is supported by Penn State MRI Nanofabrication Lab under NSF Cooperative Agreement 0335765, NNIN with Cornell University and under NSF DMR 0908700. Y.L. acknowledges partial support from Ministry of Science and Technology of China (Grant 2012CB927403) during the manuscript preparation and development of the theory. The TEM images were obtained at the TEM facility at FSU, supported by the Florida State University

Research Foundation, NSF-DMR-0654118 and the State of Florida. K.S. is supported by JQI-NSF-PFC. The work at Tulane is supported by NSF under DMR-1205469.

Author contributions

Y.L. designed the experiment; Y.A.Y., N.E.S. and X.C. fabricated the devices and performed the measurements; Y.A.Y., K.S. and Y.L. developed the phenomenological theory; Y.X. performed TEM work; D.F., T.J.L. and Z.Q.M. grew the crystals of Sr_2RuO_4. Y.A.Y. and Y.L. wrote the paper.

Additional information

Competing financial interests: The authors declare no competing financial interests.

Reprints and permission information is available online at http://npg.nature.com/reprintsandpermissions/

How to cite this article: Ying, Y. A. *et al.* Enhanced spin-triplet superconductivity near dislocations in Sr_2RuO_4. *Nat. Commun.* 4:2596 doi: 10.1038/ncomms3596 (2013).